Device Free Activity Identification Using WiFi Channel State Information Signatures

Aryan Sharma
aryans@tamu.edu
UIN - 326006767

***Abstract*—Activity monitoring in home environments now has increasing usage specially in elder care and child safety. Traditional approaches involve wearable sensors and specialized hardware installations which are intrusive as well as non-intrusive in nature. This project presents device-free location-oriented activity identification at home through the use of existing WiFi access points and WiFi devices. It takes advantage of the complex web of WiFi links between such devices and the fine-grained channel state information that can be extracted from such links. It examines channel features and can uniquely identify both in-place activities and walking movements across a home by comparing them against signal profiles.**

***Keywords*—Activity Recognition; WiFi; Device-Free; Channel State Information (CSI);**

I. Introduction

There exists a broad range of applications that benefit from higher-level contextual information, an understanding of activities that persons are engaged in, not just their position inside a coordinate system. By tracking a sequence of meaningful activities and generating statistics for a person, it is possible to monitor well-being and suggest behavioral changes that improve health, especially for children and the elderly.

This project explores and implements the *device-free* location-oriented activity identification at home through the use of existing WiFi access points and WiFi devices[2], demonstrating that device-free location-oriented activity recognition is possible (i) using the existing channel state information provided by IEEE 802.11n devices [8] and (ii) using relatively few wireless links, such as those to existing in-home WiFi devices. As a baseline this project uses the Long Short-Term Memory approach to classify activities[1] and validates the results from that experiment. The challenge in activity recognition for these applications lies in finding solutions that can provide sufficiently accurate tracking and recognition with minimal infrastructure requirements and without the need to carry a dedicated device. Other device-free systems do not require persons to carry any devices, but they require a dense placement of tens of sensors to create a mesh of wireless links inside the area of interest.

From the online repositories, the project classifies the wireless signals as belonging to an in-place or a walking activity. We refer these two types of activities as loosely-defined because they may involve non-repetitive body movements and the sequences of body movements involved may not remain the same across repetition. Examples of loosely-defined activities include cooking dinner in front of the stove, eating dinner at the dining table, exercising on a treadmill, or working at a desk.

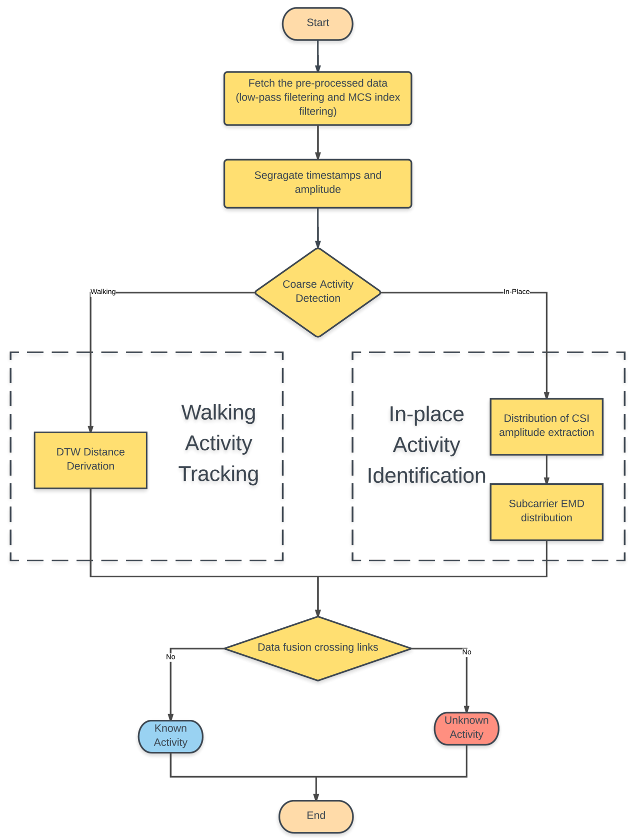

Fig. 1. Flowchart for the whole project

Walking activities involve movements between rooms or across a larger room. The system then applies matching algorithms to compare the amplitude measurements against known profiles that identify the activity. Hence, it uses data from a much smaller set of transmitting devices than traditional approaches.

II. Idea and Motivation

This project exploits two trends. First, WiFi usage is now also used to connect smart devices such as TVs, surveillance cameras, and loudspeakers to home networks and the Internet, besides providing laptop internet connectivity. An example of this arrangement is shown in Fig.2. This provides a larger number of WiFi links inside homes, some of which use constant beaconing. Second, WiFi radios provide more fine-grained channel measurements over wider bandwidths, thus providing us with more in-depth changes to the mesh formed

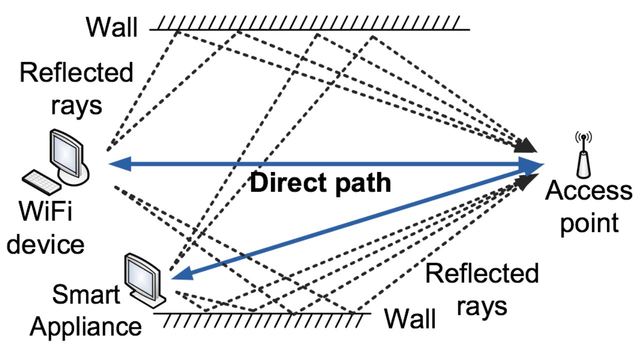

Fig. 2. CSI takes the advantage of multipath effects and captures the detailed changes on different subcarriers

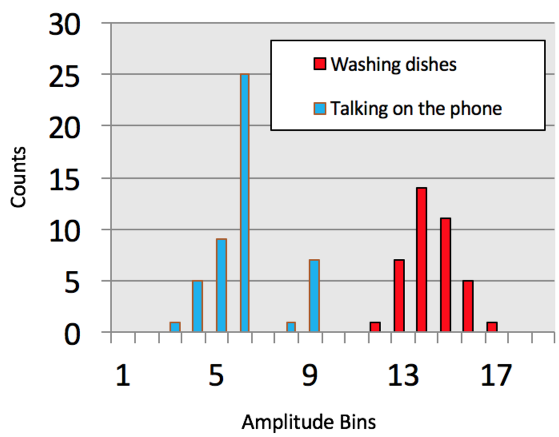

Fig. 3. Histograms of CSI amplitude of a particular subcarrier for two different in-place activities at the same position: washing dishes and talking on the phone nearby the sink.

because of these devices. Inside buildings, signal propagation is dominated by multipath, that is the received signal amplitude (or strength) is the combined amplitude of signals arriving over many different paths (scattered from and reflected off different objects).

The motivating reason why CSI data was used as a metric is explained in Figure 3. We can see the histograms for amplitude bins for two in-place activity here (talking on the phone and washing dishes). The histograms of CSI amplitudes (quantized to 20 bins) for a specific sub-carrier, however, show very distinct distributions that can clearly distinguish these different movements in the same location. The insight is that since an activity involves a series of body movements during a certain period of time, the distribution of CSI amplitudes is a desirable channel statistic that can capture unique characteristics of activities in both time and frequency domains. Given the increasing amount of Wifi devices in a typical home and ability of few APs and sensors forming a substantial mesh allows us to exploit this feature and come up with the setup.

Thus summarising, the major portions of the project are as follows and is shown as a flowchart in Fig.1:

A. *Differentiate In-Place Activities from Movements*

This project used the Channel State Information to distinguish between In-Place activity and Walking activities. These are the loosely based activities which are further classified at a finer granularity. This is owing to different levels of distortions seen in the CSI data.

B. *Detection and Classification of In-Place Activity*

The in-place activity results in a relatively stable distribution of CSI amplitude due to the presence of the human body and (possibly) repetitive body movement over time. Furthermore, different in-place activities cause different distributions of CSI amplitude as the location and/or the repetitive body movement patterns and the posture of the human body are different for different in-place activities. This difference was used to classify in-place activities.

C. *Walking Activity Tracking*

It has been shown that the CSI measurements exhibit similar changing patterns for the same trajectory in different rounds, whereas the changes of CSI measurements over time are different for different trajectories. This observation indicates that the CSI pattern is dominated by the unique path of each walking activity and this project will use it for walking activity tracking.

III. Data Collection

The experimental test-bed designed for the experiment is shown in Fig. 4. We can see one access point which is the laptop and two clients which receive the CSI data. This data is in the raw format and needs to be preprocessed. For the initial usage in this project, the data has been collected from [1] at [10]. It posses about 17 GB of data which are annotated for each of the eight activities. This data was collected using Linux 802.11n CSI Tool [8] and in the experiment. The files with ‘input_’ prefix are WiFi Channel State Information data. The files with ‘annotation_’ prefix are annotation data. In the input dataset,

- 1st column shows timestamp.
- 2nd - 91st column shows (30 subcarrier * 3 antenna) amplitude.
- 92nd - 181st column shows (30 subcarrier * 3 antenna) phase.

IV. Methodology

This project follows the flowchart shown in Figure 1. To identify activities, the system has to match signatures or features of activities to measurements in a way that is robust to noisy signal readings collected from WiFi devices in real-world environments yet are still sufficiently unique to map to a specific activity. The system takes as input time-series amplitude measurements. This data is then preprocessed to remove outliers via a low-pass filter and to filter out artifacts introduces by rate adaptation, where the radios switch to different modulation and coding scheme. This has been already done in the repository. The following steps are then applied to reach to the classification.

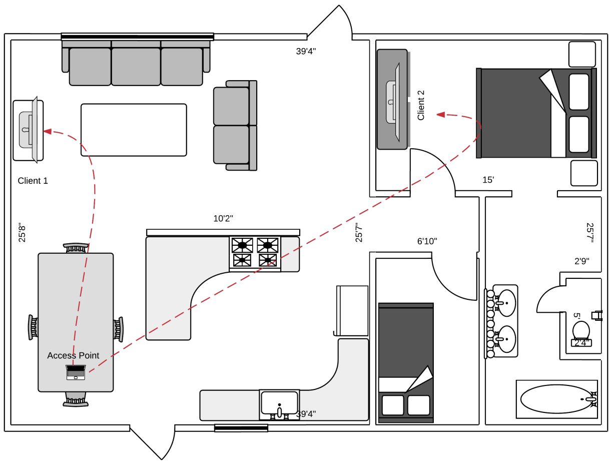

Fig. 4. Experimental test bed for data collection

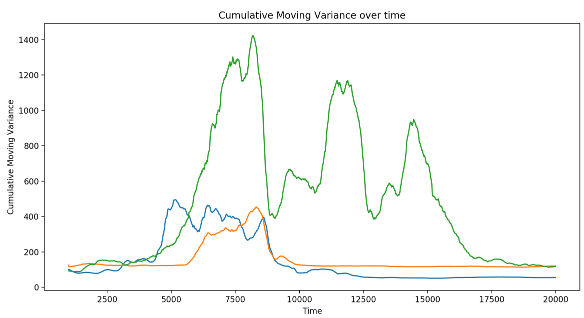

Fig. 5. Cumulative Moving Variance on three activities with time. The green line is *running*, the blue line is *washing dishes* and the orange line is *talking on the phone*

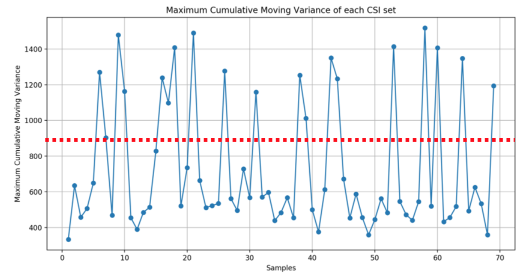

Fig. 6. Maximum Cumulative Moving Variance on all activities with time. The red line is the classifier which distinguishes between the in-place and walking activities

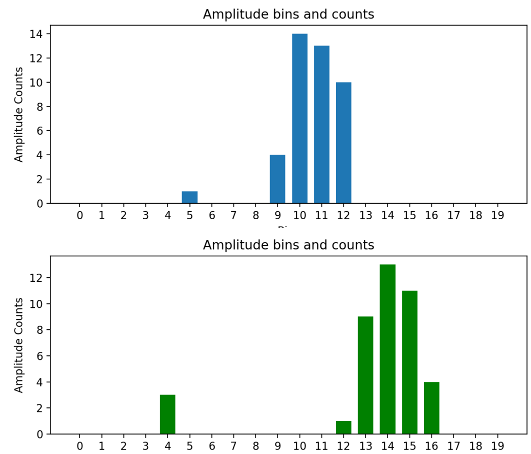

Fig. 7. Histogram of CSI amplitudes on a particular subcarrier for *Cooking (in blue)* and *Talking on the phone (in green)*

A. Coarse Activity Detection

Various activities causes different degrees of signal changes. We therefore apply the moving variance on top of the CSI measurements to capture this difference and determine the category of the activity. In particular, a large moving variance indicates the presence of a walking activity whereas a small moving variance represents the presence of an in-place activity or no activity at all. Figure 2 shows the points for large moving variance and low moving variance. The plots can be clustered into two classes. The following are the steps for this:

1. The CSI samples of P subcarriers are $C = C(1), ..., C(p), ..., C(P)$, where $C(p) = [c_1(p), ..., c_T(p)]'$ represents T CSI amplitudes on the p^{th} subcarrier. We further denote the moving variances of the P subcarriers as $V = V(1), ..., V(p), ..., V(P)$, where $V(p) = [v_1(p), ..., v_T(p)]$ are the moving variances derived from $C(P)$. The cumulative moving variance of CSI samples crossing P subcarriers as is shown in Figure 4, are calculated as, $\mathcal{V} = \sum_{p=1}^{p=P} V(p)$

2. The cumulative moving variances are the examined. If the maximum cumulative moving variance $max(V)$ is larger than the threshold τ_v , the CSI samples are determined to contain a walking activity, otherwise they contain an in-place/no activity. The value of τ_v is empirically determined.

B. In-place Activity Identification

We observe in Fig.7 that the CSI amplitude distributions are similar for the same activity at different rounds, but distinctive for different activities. This important observation inspires us to exploit the distribution of CSI amplitude to distinguish different in-place activities and shows that a particular in-place activity can be identified by comparing against known profiles.

Based on the characteristics of the in-place activities, the earth movers distance (EMD) [4] technique is employed, which is a well-known approach for evaluating the similarity between two probability distributions. The EMD has been discussed in detail in Appendix A. The EMD calculates the minimal cost to transform one distribution into the other. This classifier seeks to compare the distribution of the testing CSI measurements to those of the known in-place activity profiles by using the EMD metric. The steps are as follows:

1. At run time, it first identifies the testing CSI measurements as a candidate of a particular known in-place activity if the EMD distance from the candidate to the known in-place activity is the minimum among

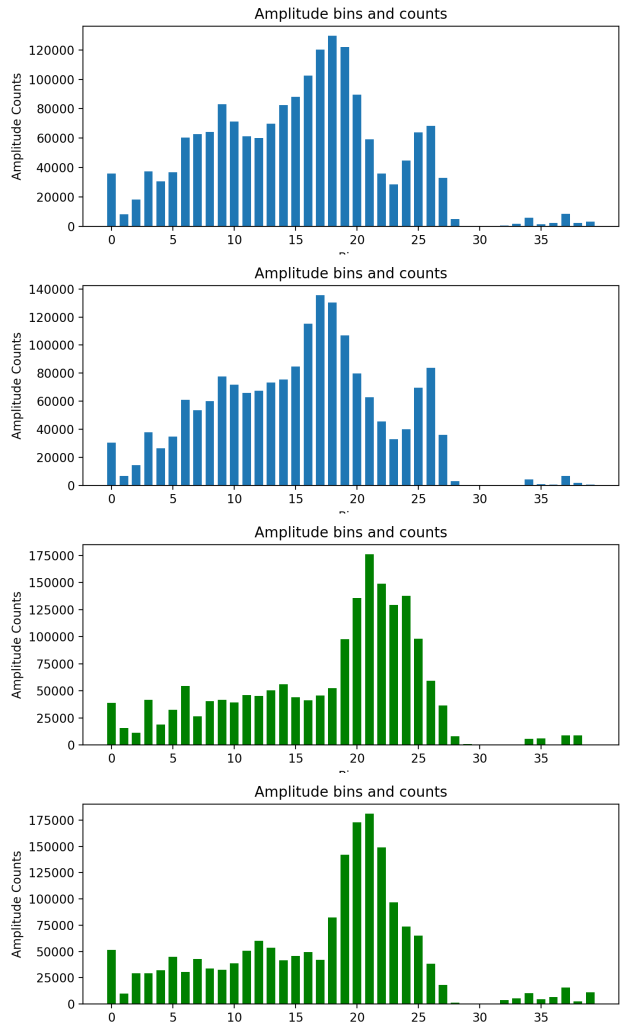

Fig. 8. Amplitude counts in the bins for *Running (in blue)*and *Walking (in green)* for different rounds. As we can see that the distributions hardly changed for two rounds of recording data for the same locomotion involving activity

the EMD distances to all known activities stored in the CSI profiles.

2. Then it further confirms the candidate known in-place activity by comparing the resulted minimal EMD distance to a threshold, which can be empirically determined. The candidate known in-place activity is confirmed if the minimal EMD distance is less than the threshold, otherwise, it will be identified as an unknown activity.

C. Walking Activity Tracking

The CSI measurements exhibit similar changing patterns for the same trajectory in different rounds, whereas the changes of CSI measurements over time are different for different trajectories. This observation indicates that the CSI pattern is dominated by the unique path of each walking activity and is shown in Fig.8.

To do the Walking Path Discrimination, Dynamic Time Warping (DTW) is used. This also takes into account the different speed taken by people for the same path. DTW is to

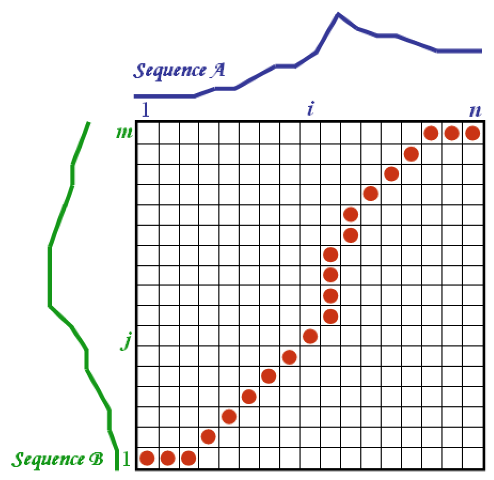

Fig. 9. DTW finds the minimum distance to convert one sequence to another using a dynamic approcah. The path taken as shown in the figure is the minimum cost path. The summation of the path is the total cost.

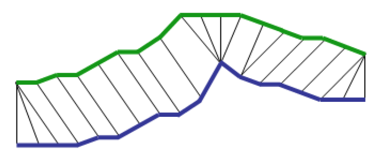

Fig. 10. This figure shows the corresponding warping from the DTW for two sequences

align the testing CSI measurements to those of known activities in the profile. DTW stretches and compresses required parts to allow a proper comparison between two data sequences. This is useful to match CSI samples from different walking speeds in real-world scenarios. For multiple sub-carrier groups, Multi-Dimensional Dynamic Time Warping (MD-DTW) is used. The steps that will be followed are as follows and a graphical visualization is shown in Fig.9 and 10 for the MD-DTW approach.

1. The vector norm is utilized to calculate the distance matrix according to the following equation: $d(c_i, c_j^{'} = \sum_{p=1}^{P}(c_i(p) - c_j^{'}(p))^2$, where $C = c_1, c_2, ..., c_T$ and $C^{'} = c_1^{'}, c_2^{'}, ..., c_T^{'}$ are two sequences for walking path discrimination, and where P is the number of dimensions of the sequence data.
2. A least cost path is found through this matrix and the MD-DTW distance is the sum of matrix elements along the path.
3. During activity identification, this system distinguishes each walking activity by calculating the MD-DTW distance between the testing CSI measurements and all the known walking activities in CSI profiles. It then stores the segment of CSI measurements of known activities in profiles. If the MD-DTW distance is less than a threshold (i.e., considering it as a known activity), we then regard the corresponding CSI measurements labeled in the CSI profiles with the minimum distance as the activity identified for the testing measurements.

	a	b	c	d	e	f	g	h	unknown
a: empty	1	0	0	0	0	0	0	0	0
b: cooking	0	0.93	0.02	0.05	0	0	0	0	0
c: eating	0	0	1	0	0	0	0	0	0
d: washing dishes	0	0.12	0	0.88	0	0	0	0	0
e: typing	0	0	0.01	0	0.99	0	0	0	0
f: brushing	0	0	0	0.05	0	0.95	0	0	0
g: bathing	0	0	0	0	0	0.08	0.92	0	0
h: walking/running	0	0	0	0	0	0	0	1	0
o: others	0	0	0	0	0	0	0	0	1

Actual Activity

Identified Activity

Fig. 11. Results shown in a Confusion Matrix

D. Data Fusion Crossing Multiple Links

For the data that we have, we can use, multiple access points to improve the activity recognition accuracy based on the basic schemes.

Assuming L WiFi devices collecting CSI measurements independently and each device having J activity profiles denoted as $a_1^l, ..., a_j^l, ..., a_J^l, l = 1, ..., L$. The final activity recognition result is the j^{th} activity (profile) that minimizes the weighted summation of the similarities between the collected CSI measurements and the profiles on each WiFi device, i.e.,

$$a_j^* = \underset{j}{\operatorname{argmin}} \sum_{l=1}^{L} [w_l^j(a_0^l, a_j^l) * D_j^l]$$

where D_j^l is the EMD or DTW distance between the CSI measurements and the j^{th} activity profile on the l^{th} WiFi device; $w_j^l(a_l^0, a_l^j)$ is the normalized weight dominated by the significance of the jth activity on the l^{th} WiFi device. It is defined as,

$$w_j^l(a_l^0, a_l^j) = \frac{1 - \chi(a_0^l, a_j^l)}{\sum\limits_{l=1}^{L} 1 - \chi(a_0^l, a_j^l}$$

where a_0^l denotes the profile for empty room on the l^{th} WiFi device, and $\chi(a_0^l, a_j^l)$ is the cross correlation between the profile of the empty room and the jth activity on the l^{th} WiFi device.

V. Results and Conclusion

The classifier was able to successfully seggregate walking/running activities from other activities. The other in-place activity were detected with good accuracy. The result has been tabulated into a Confusion matrix, shown in Fig.11.

Each row represents the actual activity performed by the user and each column shows the activity it was classified as by our system. Each cell in the matrix corresponds to the fraction of activity in the row that was classified as the activity in the column. As can be seen in the results, certain activities which occured in the common locations are misplaced or have a very similar body movements. Examples are cooking and washin dishes, bathing and brushing etc.

Appendix A
Earth Mover's Distance

The Earth Mover's Distance (EMD) is a useful metric between two signal signatures. The main difference between EMD and Euclidean based approaches is that we solve the EMD problem which finds the optimal match between two distributions where variable-sized pieces of mass are allowed to be moved together in contrast to the matching problem where unit elements of fixed size are matched individually. This distinction significantly increases efficiency due to the more compact representation as a result of clustering data in the feature space. In our project we used this to ascertain which activity histogram correlates the most with the given known activity histograms.

The EMD is based on the following linear programming problem: Let $P = (p_1, w_{p1}), ..., (p_m, w_{pm})$ be the first signature with m clusters, where p_i is the cluster representative and w_{pi} is the weight of the cluster; $Q = (q_1, w_{q1}), ..., (q_m, w_{qm})$ the second signature with n clusters; and $D = [d_{ij}]$ the ground distance matrix where $d_{ij} = d(p_i, q_j)$ is the ground distance between the clusters p_i and q_j.

We want to find a flow $F = [f_{ij}]$ with f_{ij} the flow between p_i and q_j, that minimizes the overall cost

$$WORK(P, Q, F) = \sum_{i=1}^{m} \sum_{j=1}^{n} d(p_i, q_j) f_{ij}$$

subject to the following constarints:

$$f_{ij} \geq 0, \qquad 1 \leq i \leq m, 1 \leq j \leq n$$

$$\sum_{j=1}^{n} f_{ij} \leq w_{pi}, \qquad 1 \leq i \leq m$$

$$\sum_{i=1}^{m} f_{ij} \leq w_{pj}, \qquad 1 \leq i \leq n$$

$$\sum_{i=1}^{m} \sum_{j=1}^{n} f_{ij} = min(\textstyle\sum_{i=1}^{m} w_{pi}, \sum_{j=1}^{n} w_{pi})$$

Constraint 1 allows moving supplies from P to Q and not vice versa. Constraint 2 limits the amount of supplies that can be sent by the clusters in P to their weights. Constraint 3 limits the clusters in Q to receive no more supplies than their weights; and Constraint 4 forces the maximum amount of supplies possible to be moved. We call this amount the *total flow*. Once the transportation problem is solved and we have found the optimal flow F, the Earth Mover's Distance is defined as the resulting work normalized by the total flow,

$$EMD(P, Q, R) = \frac{\sum\limits_{i=1}^{m} \sum\limits_{j=1}^{n} d(p_i, q_j) f_{ij}}{\sum\limits_{i=1}^{m} \sum\limits_{j=1}^{n} f_{ij}}$$

The normalization factor is the total weight of the smaller signature, because of constarint 4. This factor is needed when two signatures have different total weights in order to avoid favoring smaller signatures.

Appendix B
Dynamic Time Warping

In recent years Dynamic Time Warping (DTW) has emerged as the distance measure of choice for virtually all time series data mining applications. DTW is in-fact faster than all but the most carefully optimized implementations of Euclidean Distance now. In this section we describe how the DTW gives us the distance between two CSI measurements.

Each CSI measurement is a *Time Series*, which is defined as $T = t_1, t_2, ..., t_n$, which is an ordered set of real values. The total number os real values is the length of the time series. A dataset $D = \{T_1, T_2....T_m\}$ is a collection of M such time series. A *Multidimensional Time Series* (MDT) consists of M individual time series ($M \geq 2$), where wach time-series has n observations:

$Q_1 = q_{1,1}, q_{1,2}, q_{1,3}, q_{1,4}, ..., q_{1,n},$

$Q_2 = q_{2,1}, q_{2,2}, q_{2,3}, q_{2,4}, ..., q_{2,n},$

.....

$Q_M = q_{M,1}, q_{M,2}, q_{M,3}, ..., q_{M,n}$

If we wish to compare two time series, we could use the ubiquitous Euclidean distance. However, the DTW distance subsumes the Euclidean distance as a special case. Unlike the Euclidean distances strict one-to-one alignment, DTW allows a one-to-many alignment, as illustrated in Fig.9. To align sequences using DTW, an n-by-n matrix is constructed with the (i^{th}, j^{th}) element being the squared Euclidean distance $d(q_i, c_j)$ between the points q_i and c_j. A warping path P is a contiguous set of matrix elements defining a mapping between Q and C. The t^{th} element of P is defined as $p_t = (i, j)_t$, so we have:

$$P = p_1, p_2, p_3, p_4, ..., p_T \qquad n \leq T \leq 2n - 1$$

The warping path that defines the alignment between the two time series is usually subject to several constraints: the warping path must start and finish in diagonally opposite corner cells of the matrix, the steps in the warping path are restricted to adjacent cells, and the points in the warping path must be monotonically spaced in time. In addition, virtually all practitioners using DTW also constrain the warping path in a global sense by limiting how far it may stay away from the diagonal.

While there are exponentially many warping paths that satisfy the above constraints, we are only interested in the path that minimizes the warping cost:

(1) $DTW(Q, C) = min(\sqrt{\sum_{t=1}^{T} p_t})$

This path can be found using dynamic programming to evaluate the following recurrence (Fig. 8), which defines the cumulative distance $D(i, j)$ as the distance $d(i, j)$ found in the current cell and the minimum of the cumulative distances of the adjacent elements.

(2) $D(i, j) = d(q_i, c_j) + min\{D(i-1, j-1), D(i-1, j), D(i, j-1)\}$ where, $d(q_i, c_j) = (q_i - c_j)^2$

The DTW distance as showed is applicable only to one dimensional case, we extend it for multi-dimensional case in two manner. One is the *independent* DTW, designated as $DTW_I$and other is *dependent* DTW, designated as DTW_D.

DTW_I is the cumulative distances of all dimensions independently measured under DTW. If $DTW(Q_m, C_m)$ is defined as the DTW distance of the m^{th} dimension of Q and the m^{th} dimension of C, we can write DTW_I as:

(3) $DTW_I(Q, C) = \sum_{m=1}^{M} DTW(Q_m, C_m)$

In the above equation, each dimension is considered as independent and DTW is allowed the freedom to warp each dimension independently of the others.

DTW_D is calculated in a similar way to DTW for single-dimensional time series, except that we redefine $d(q_i, c_j)$ as the cumulative squared Euclidean distances of M data points instead of the single data point used in the more familiar one-dimensional case. Formally, if $q_{i,m}$ is the i^{th} data point in the m^{th} dimension of Q and $c_{j,m}$ is the j^{th} data point in the m^{th} dimension of C, we replace $d(q_i, c_j)$ in Eq. (2) with:

(4) $d(q_i, c_j) = \sum_{m=1}^{M} (q_{i,m} - c_{j,m})^2$

References

[1] S. Yousefi, H. Narui, S. Dayal, S. Ermon, and S. Valaee'A Survey on Behaviour Recognition Using WiFi Channel State Information'

[2] Y. Wang, J. Liu, Y. Chen, M. Gruteser,'E-eyes: Device-free Location-oriented Activity Identification Using Fine-grained WiFi Signatures'

[3] Ofir Pele and Michael Werman, 'Fast and robust earth mover's distances,' in Proc. 2009 IEEE 12th Int. Conf. on Computer Vision, Kyoto, Japan, 2009, pp. 460-467.

[4] Y. Rubner and S. U. C. S. Dept. Perceptual metrics for image database navigation. Number 1621 in Report STAN-CS-TR. Stanford University, 1999.

[5] Ofir Pele and Michael Werman, 'A linear time histogram metric for improved SIFT matching,' in Computer Vision - ECCV 2008, Marseille, France, 2008, pp. 495-508.

[6] W. Wang, . X. Liu, and M, Shahzad, K. Ling, and S. Lu, 'Device-Free Human Activity Recognition Using Commercial WiFi Devices'

[7] http://pdcc.ntu.edu.sg/wands/Atheros/

[8] https://dhalperi.github.io/linux-80211n-csitool/

[9] https://stackoverflow.com

[10] https://stanford.app.box.com/s/johz79hz7n2jue5biqlxja6vbq7xtk9l